Transcriptional Regulation of Members of the Tripartite Motif Family in Response to Viral Infection

Benjamin Tseng

April 2007

Abstract

TRIM30 and TRIM34 are two proteins of the Tripartite Motif family which have recently been shown to be dependent on IKKε, a kinase implicated in the regulation of a subset of genes critical for innate immunity, for their proper transcriptional regulation. This study performs a functional analysis of the genes and finds evidence that the two genes help mediate a host cell's antiviral state. This study also characterizes the transcriptional regulation of these genes finding that they are dependent on the cytokine Interferon β and on the Interferon β activated kinase IKKε for proper upregulation. The nature of this transcriptional regulation is tracked to a specific Interferon Stimulated Response Element in their promoter, and this evidence is used to conjecture based on network motif analysis the role of this and other genes involved in the host cell response to viral infection.

Contents

List of Figures

List of Tables

Statement of Research

This thesis was undertaken in the laboratory of Professor Tom Maniatis of the Department of Molecular and Cellular Biology at Harvard University and is a culmination of work done from February 2006 to April 2007. It was conducted under the direct supervision of Postdoctoral Fellow Dr. Benjamin tenOever.

Acknowledgements

I would like to thank Professor Maniatis for his generous donation of time and resources to this endeavor. I would also like to thank the various members of the Maniatis lab for countless hours of time and countless words of encouragement. Specifically, Sze-Ling Ng and Nan Zhu deserve special praise for their patience and support. I would also like to extend my sincerest gratitude to Benjamin tenOever whose patience, enthusiasm, and guidance made this one of the most worthwhile and educational experiences I have had.

Introduction

Cellular Response to Viral Infection

Eukaryotic cells face a constant barrage of intracellular pathogens. While a system-wide immune response consisting of multiple cellular and humoral effectors ultimately clears infection, the initial cellular response to infection has been found to be critical not only in slowing the initial progression of disease but also in activating the larger system-wide response. It has been demonstrated that cells infected by virus induce a multitude of responses designed to inhibit critical junctions in the viral lifecycle. The regulation of this diverse set of responses converges on the regulation and expression of the Interferon (IFN) family of proteins (*1*). The IFNs can be classified broadly into two categories: the type 1 IFNs (e.g. IFNβ) and the type 2 IFNs (e.g. IFNγ). While receptors for both exist in a wide variety of cell types, the type 2 IFNs are only produced by a restricted subset of immune cells (i.e. antigen-presenting cells [APCs] and lymphocytes) and primarily function in an immunomodulatory capacity (*2*). In contrast, IFNβ is produced by a wide range of cells in response to pathogenic insult and functions as the cytokine of greatest import to inducing an antiviral state (*3*).

The events leading to IFNβ activation have been studied extensively. There are two major modes of activation, stemming from two major modes of viral detection — one used primarily by specialized APCs and another by infected cells (*4, 5*). APCs employ germline coded Toll-like Receptors (TLRs) to recognize pathogen-associated molecular motifs which signify the presence of infection. In the case of viruses, a battery of TLRs recognize viral replication intermediates such as ssRNA (TLR7), dsRNA (TLR3), and unmethylated CpG islands (TLR9). Infected non-APCs, on the other hand, typically employ the cytosolic RNA helicases Retinoic acid-Inducible Gene-I (RIG-I) and Melanoma Differentiation Associated gene 5 (MDA5) to detect a wide range of RNA viruses (*6*).

Downstream of this detection event, a large transcriptional structure called the Enhanceosome assembles on the enhancer of the IFNβ gene (Figure 1a) (*7*). This complex consists of the transcription factors Nuclear Factor κB (NF-κB), heterodimers and homodimers of IFN Regulatory Factor 7 (IRF7) and IRF3, and the Activation Protein complex-1 (AP-1). These factors are in turn activated by the canonical IκB (Inhibitor of NF-κB) Kinases (IKKα and IKKβ) which mediates the targeted degradation of IκB (*8*), the non-canonical IKK kinases Tank-Binding Kinase 1 (TBK1) and IKKε which phosphorylate IRF3 and IRF7 (*9, 10*), and the c-Jun N-terminal Kinase (JNK) which phosphorylates the components of AP-1 (*8*). The activated forms of these transcription factors translocate to the nucleus and bind to DNA sequences called Positive Regulatory Domains (PRDs) upstream of IFNβ in a cooperative fashion involving the High Mobility Group protein (HMG-I) which induces an architectural remodelling of the DNA in a way which is conducive to enhanceosome binding cooperativity.

The specific pathway connecting the initial viral detection event and enhanceosome binding depends on the mechanism of initial viral detection (*5, 11, 12*). Signaling through TLR7 and 9 in APCs leads to the recruitment of the adaptor molecule MyD88 which in turn recruits family members of the IL-1 Receptor Associated Kinases (IRAK1 and IRAK4). These kinases phosphorylate and activate the E3 Ubiquitin ligase TRAF6 (TNF Receptor Associated Factor 6) and IRF7. TRAF6 then ubiquitinates the NF-κB Essential Modulator (NEMO/IKKγ), providing an activation signal to NF-κB, and recruits the TGFβ Activated Kinase 1 (TAK1) complex. TAK1 can then phosphorylate IKKβ and members of the MAP Kinase Kinase family upstream of JNK activation.

Signaling through TLR3, on the other hand, employs a MyD88-independent signaling pathway (*5, 11, 12*). Activated TLR3 recruits the adaptor TRIF. TRIF can activate NF-κB and JNK through interaction with TRAF6 and the Receptor Inter-

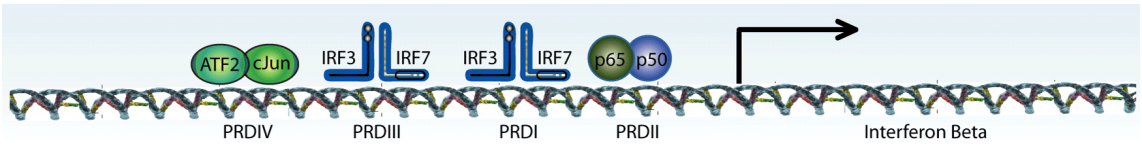

(a) Interferon Beta Enhancer

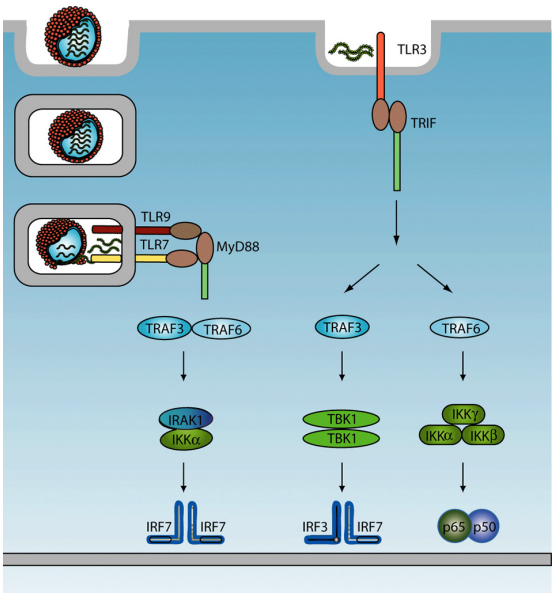

(b) Viral Detection through TLRs

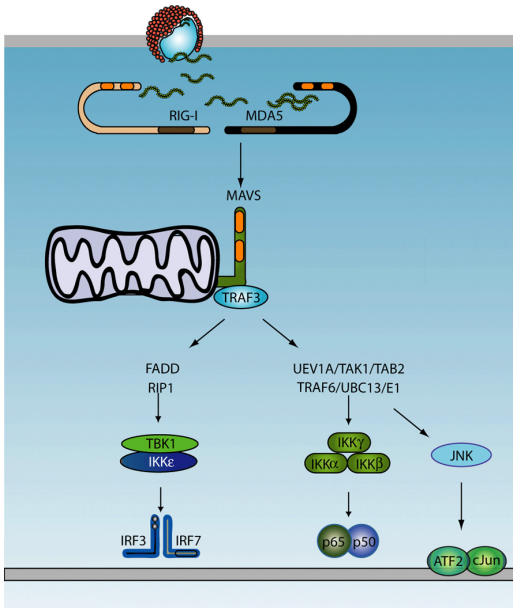

(c) Viral Detection through RNA Helicases

Figure 1: **Viral detection leads to Interferon Beta upregulation.** Upon detection of viral molecular motifs, downstream signaling pathways activate the individual components of NF-κB, the IRFs, and AP-1 which then bind cooperatively to the IFNβ promoter.

acting Protein-1 (RIP1), which acts on IKKβ. TRIF also directly associates with and activates TBK1, thus inducing the phosphorylation of IRF3 and IRF7 in this pathway (Figure 1b).

In non-APCs, the cytosolic RNA helicases RIG-I and MDA5 detect RNA viral replication intermediates as a sign of infection (*13*). The subsequent activation of IFNβ is mediated through the Mitochondrial AntiViral Signaling protein (MAVS) which has also been termed Cardif, IPS-1, and VISA (*14–17*). MAVS, which is located on the outer mitochondrial membrane, is thought to interact with the RNA helicases upon viral detection through Caspase Recruitment Domain (CARD) interactions and mediates IFNβ upregulation by association with TRAF3 which has recently been found to be associated with TRIF, IRAK-1, TBK1, and IKKε and hence upstream

of the events needed for IFNβ upregulation (Figure 1c) (*18, 19*).

The "Noncanonical" IKK Kinases

TBK1 and IKKε are oftentimes termed the "noncanonical" IKK kinases or the IKK-related kinases, as opposed to the canonical IKK kinases IKKα and IKKβ which they share a reasonable degree of sequence homology with (*20*). TBK1 was originally identified by three groups, two who made the identification based on its association with TANK, a protein associated with the adaptor protein TRAF (*21, 22*), and one based on its ability to activate NF-κB by acting upstream of the IKK$\alpha/\beta/\gamma$ complex (*23*). IKKε was identified by two groups, one who made the identification based on a database search for kinases similar to IKKα and IKKβ (*24*) and the other based on identifying genes upregulated by lipopolysaccharide treatment (*25*). It is not surprise that early investigations of TBK1 and IKKε focused on their roles in modulating NF-κB activity via their activity vis-a-vis the IKK complex.

It was later found that TBK1 and IKKε play a major role in the phosphorylation of IRF3 and IRF7 (*9, 10, 26*). However, while mice deficient in TBK1 or in both TBK1 and IKKε showed severe problems with IFNβ induction in response to immunological stimuli, mice deficient only in IKKε showed no severe defect in IFNβ induction (*27*). This result suggested that the two kinases played redundant roles with TBK1 playing the dominant role in the phosphorylation of IRF3 and IRF7 leading up to IFNβ upregulation and IKKε playing a more auxillary one.

Interferon Signaling

Following enhanceosome binding, IFNβ is secreted by the APC or infected cell into the neighboring environment. It then binds in an autocrine and paracrine fashion to cell surface receptors consisting of IFNAR1 and IFNAR2 which mediate all of Type 1 IFN signaling (*1*). Binding of IFN to these surface receptors induces receptor

dimerization whereby the Janus Kinases associated with IFNAR1 and IFNAR2, Tyk2 and Jak1 respectively, phosphorylate each other and IFNAR1 at well-defined tyrosine residues. These phosphorylated tyrosines recruit the Signal Transducers and Activators of Transcription proteins STAT1 and STAT2 via their Src-Homology 2 (SH2) domains. STAT1 and STAT2 are themselves then phosphorylated by the IFNAR-associated kinases.

The phosphorylation of STAT1 and STAT2 on tyrosine residues enable the proteins to interact with each other through their SH2 domains, generating two transcriptionally active structures. Homodimers of phosphorylated STAT1, also referred to as IFNα Associated Factor (AAF), translocate to the nucleus and bind to IFNγ Activation Site (GAS) elements (*28*). Trimers of phosphorylated STAT1, phosphorylated STAT2, and IRF9, also referred to as IFN Stimulated Gene Factor-3 (ISGF3), translocate to the nucleus and bind to IFN Stimulated Response Elements (ISREs) (*29, 30*). These events lead to the upregulation of a battery of IFN Stimulated Genes (ISGs) which mediate the antiviral state induced by IFN (*3*).

A recent study shows that IKKε, which was formerly believed to only function as a redundant kinase for IRF3 and IRF7, plays a major role in the regulation of IFN signaling (Figure 2) (*31*). Cells deficient in IKKε, while expressing a normal phenotype with regards to IRF3/7 phosphorylation and IFN production, showed defects in the induction of a subset of ISGs, including the dsRNA-activated Adenosine Deaminase (ADAR) gene, in response to IFNβ stimulation. Mice lacking IKKε, although not suffering from any deficiency in adaptive immunity, show a greater susceptibility to viral infection. The molecular mechanism for this was found to be an inability of ISGF3 to bind the ISREs of the affected subset of genes, most of which lacked a purine-rich tract flanking one side of the ISRE. The study determined that IKKε phosphorylates STAT1, a post-translational modification believed to alter the structure of ISGF3, allowing ISGF3 to bind ISREs lacking the purine-rich tract. The specific phenotype

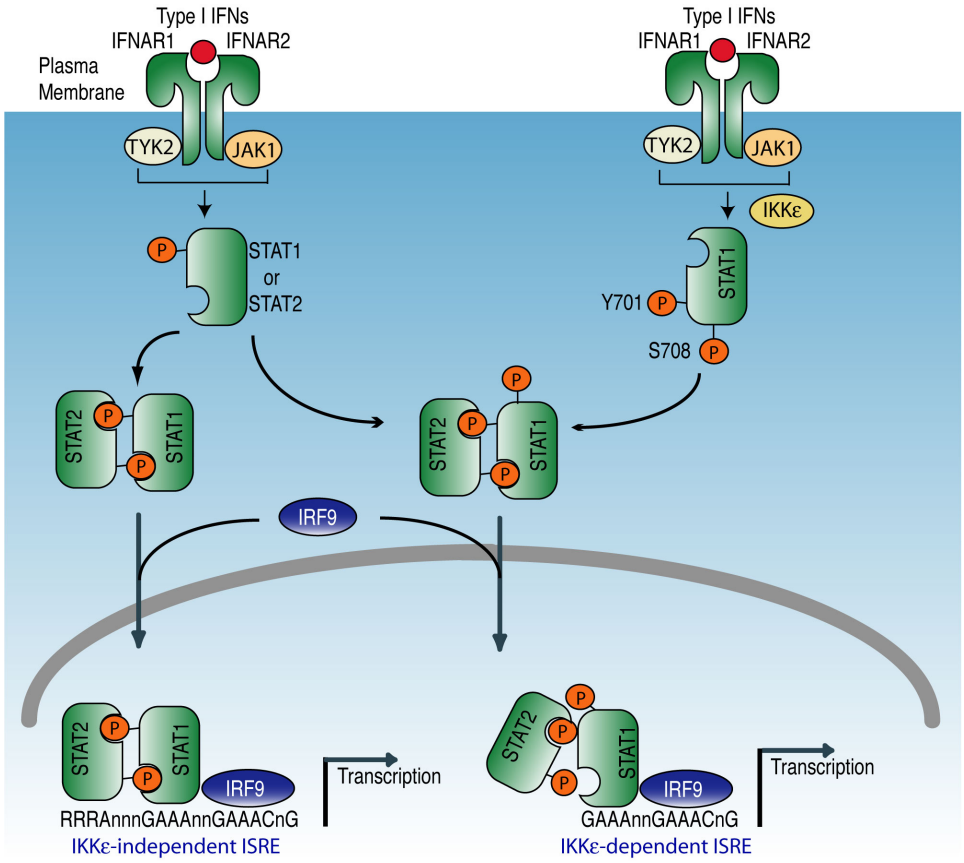

Figure 2: **IKKε directs ISGF3 binding.** IFN signaling leads to the formation of ISGF3. One of its components, STAT1, is phosphorylated at Serine 708 by IKKε, a modification which allows ISGF3 to bind to a subset of ISREs which are unable to bind ISGF3 containing an unphosphorylated form of STAT1.

of the IKKε knockout mice thus led to the speculation that IKKε regulates the set of ISGs directly associated with maintaining an antiviral state while leaving intact the system of responses integrating the innate immune response to the wider systemic one.

Tripartite Motif Family

The Tripartite Motif (TRIM) family of proteins encompasses a wide range of proteins which are responsible for functions that are only now beginning to be elucidated (*32, 33*). The defining trait of the family is the characteristic presence of a RING Domain, followed by one or two B-Box Domains, and a stretch of amino acids forming

Coiled-Coil structures, a sequence called the RBCC or tripartite motif. The C2 RING domain found on TRIM proteins employs a "cross-brace" system of cysteines and histidines to coordinate two Zinc ions (*34*). This domain has been found to be associated with ubiquitination. It has thus been hypothesized that many members of the TRIM family are E3 Ubiquitin Ligases — a fact that has been confirmed for several TRIM proteins.

The B-Box domains are also suspected to function as Zinc ion coordinators, a property confirmed by structural NMR studies (*35–37*). There are two general classes of B-box domains. B-box1 also adopts the "cross-brace" system analogous to that employed by the RING domain and is thus able to chelate two Zinc ions. B-box2, however, can only chelate one Zinc ion. Although no ascribed function for these domains has been validated, TRIM protein B-Box domains show very strong adherence to their consensus sequence, and TRIM proteins either contain both B-box1 and B-box2 domains or contain only a B-box2 domain, suggesting an importance for the domain.

The Coiled-coil structure shows the greatest variability of the conserved tripartite motif. It is oftentimes composed of two or three smaller coiled-coil regions. The region does not show any strong consensus except for hydrophobic residues such as Leucine in areas to facilitate the "knobs in holes" coiled-coil stacking structures, suggesting that the coiled-coil structures are used for homo-oligomerization. It has also been suggested that cellular localization is disrupted by the disruption of the coiled coil region (*38*).

The amino acids C-terminal to the RBCC motif show great diversity among the family members and even between splice variants of the same gene, suggesting that the conserved RBCC motif provides a specific functional role which is targeted by the C-terminus (*32, 33*). Despite the great variation in C-termini composition, the C-termini of the various TRIM proteins do show certain recurrent motifs. One of

TRIM	Protein Name	Function
1	Mid2	Viral restriction
5α		Viral restriction
5α-CypA		Viral restriction
8	GERP	Degradation of SOCS-1
19	PML	Formation of Nuclear Bodies; Viral restriction
22	Staf50	Transcriptional repression of viral genes
25	Efp	Ubiquitination of RIG-I, ISG15-ylation
27	Rfp	Inhibition of IKK kinases
30	Rpt1	Transcriptional repression?
32	HT2A	Transcriptional repression of viral genes
34	Rnf21, IFP1	Interferon stimulated gene
45		Transcriptional repression

Table 1: **Many TRIM proteins exhibit immunological properties.**

the most common is the B30.2/SPRY domain which is found in almost two-thirds of the known TRIM species. NHL repeats, ARF domains, PHD-BROMO domains, and MATH domains have also been found. To date, the functional importance of these motifs is not well-understood and not easily generalizable.

Immunological Functions of TRIMs

Many TRIM proteins now have immunological functions ascribed to them (Table 1) (*33*). This is not surprising as ubiquitin-mediated degradation and ubiquitin-mediated activation is a key step in many immune pathways (*39*). One of the most studied of the immunological TRIMs is TRIM19, an ISG (*40*) also known as the Promyelocytic Leukemia protein (PML). Various studies have found that TRIM19 expression modulates the susceptibility of a cell to various retroviruses. Although the precise mechanisms have yet to be elucidated and accounts have been divergent, it is believed that this property stems from TRIM19's SUMOylation which targets the protein to nuclear bodies and induces its degradation (*41*) as disruption of this appears to abrogate TRIM19's antiviral effects .

TRIM5α has recently received a great deal of attention for its ability to mediate

the so-called "Lv1 restriction" of a number of viral strains including HIV-1 in certain primate species. This viral restriction is believed to be mediated through an interaction with the viral capsid protein and has been mapped to the C-terminal SPRY domain as a single point mutation at residue 322 from proline to arginine was found to confer upon human TRIM5α an ability to restrict HIV infection (*42*). Interestingly, owl monkeys express a TRIM5α-CyclophilinA (TRIM5-Cypa) fusion protein where the Cyclophilin A moiety replaces the SPRY domain. TRIM5-CypA, however, can still mediate viral (including HIV-1) restriction, and this activity has been linked to its ability to bind viral capsid proteins (*43*). It is also interesting to note that mutations which abrogate the RING domain's ability to mediate ubiquitination reduce TRIM5α's ability to restrict viral infection (*44*).

Several other TRIMs have also exhibited viral restriction. TRIM1 has been linked to the restriction of murine leukemia virus. Studies have also shown that TRIM32 and the ISG TRIM22, also known as Staf50, can mediate transcriptional repression of HIV-1 genes by interaction with the Tat proteins and with HIV-1's long-terminal repeats, respectively.

TRIM family proteins have also been found to play immunological roles other than direct viral restriction. TRIM proteins which reduce immune signaling include TRIM45, which has been implicated in repressing the transcriptional activity of AP-1 (*45*), and TRIM27, which was found to interact with and repress the activities of IKKα, IKKβ, IKKε, and TBK1 (*46*). Other TRIMs serve to enhance the immune response. TRIM8 has been found to ubquitinate and target for degradation the Suppressor of Cytokine Signaling-1 (SOCS-1), a protein responsible for shutting down IFNγ signaling (*47*). TRIM25 has been experimentally demonstrated to mediate the covalent attachment of ISG15, an IFN-stimulated ubiquitin-like molecule, to various substrates including itself (*48, 49*). A recent study published this month has also linked TRIM25 to the viral detection pathway mediated by the RNA he-

licase RIG-I (*50*). The study demonstrated that the C-terminal SPRY domain of TRIM25 can directly interact with the CARD domains of RIG-I which mediate RIG-I's interaction with MAVS. Following this interaction, TRIM25 ubiquitinates RIG-I which then increases its downstream signaling activity vis-a-vis MAVS as shown by the greatly compromised ability of cells to fight off viral infection and produce IFNβ in TRIM25-deficient cells.

This report focuses on the functions and transcriptional regulation of TRIM30 and TRIM34, two ISGs that were found to be dependent upon IKKε for their proper induction (*31*). Although a previous study suggested that TRIM30 (also referred to as Rpt-1) was expressed in helper T-cells as a regulator of IL-2 and HIV-1 transcription (*51*), this work has not been followed up. Similarly, although a previous study has established that TRIM34 (also referred to as Rnf21 and IFP1) is an ISG, its function and mechanism of action have yet to be elucidated.

Materials and Methods

Reagents and Antibodies

Poly dI-dC and Lipofectamine 2000 were purchased from Amersham. Antibodies to FLAG (Sigma, Mouse IgG), GFP (Molecular Probes, Rabbit IgG), C/EBPα (Santa Cruz, sc-61, Rabbit IgG), STAT1α (Santa Cruz, sc-417, Mouse IgG), and STAT2 (Santa Cruz, sc-950, Rabbit IgG) were purchased from their respective vendors. Recombinant IFNβ was obtained from Sigma and used at a final concentration of 0.01 units/mL. Double stranded RNA (polyinosinic-cytidylic acid) was obtained from Sigma.

Viruses and Cell Culture

Sendai Virus (Strain 52) and Vesicular Stomatitis Virus (Indiana) were gifts to the Maniatis Lab from Professor Adolfo Garcia-Sastre. Sendai virus was propagated in fertilized eggs and titer determinations were made via plaque assay. Vesicular Stomatitis Virus was propagated in Vero cells. Mouse embryonic fibroblasts were grown in Dulbecco's Minimal Essential Medium supplemented with 10% heat-inactivated fetal bovine serum. *Ex vivo* infections were performed in cell culture by adding virus directly to the media at an MOI of 0.1. IFNβ treatment was performed by adding IFNβ at a concentration of 0.01 units/mL directly to the media. Transfections and treatment with double stranded RNA (dsRNA) were done using Lipofectamine 2000 per manufacturer's instructions.

Deletion of IKKε in mice was accomplished through standard homologous recombination and selection techniques by Benjamin tenOever (*31*). All cells employed were derived from mice homozygous for the absence of IKKε. Sv129 fibroblasts expressing IFNAR1 with a disrupted exon 3 were a gift to the Maniatis Lab from Professor Kate Fitzgerald.

RT-PCR

RNA was extracted from whole cells with Qiagen's RNeasy kit. Two micrograms of extracted RNA was then reverse transcribed with Superscript III Reverse Transcriptase (Invitrogen) using oligo-dT primers at 50 C for one hour and then diluted ten-fold in water. One-fortieth of the prepared cDNA was then subjected to PCR reactions using High Fidelity Taq Polymerase (Roche) with a final total primer concentration of 1 μM employing 27 cycles unless otherwise noted. PCR products were run out on 2% agarose gels stained with 0.004% (by volume) Ethidium Bromide. Primers employed are listed in Table 2.

Primer Set	Forward Primer: 5' to 3'	Reverse Primer: 5' to 3'
HPRT	ACCTCCTCCGCCGCCTTCC	GCCCCCCTTGAGCACACAGAG
IFNβ	GTCTCATTCCACCCAGTGCT	CAGCTCCAAGAAAGGACGAA
IKKε	CGCAAACCCCAGCAAAAGGC	TCTTCCACCTCCAGGATGTTGGC
IFNAR1	TGGAAATACCTGTGTCATGTGTGCTTCC	AAACACCGAGACAGAACCACCAGATGCC
IFNAR1 exon 3	AAGATGTGCTGTTCCCTTCCTCTGCTCTGA	ATTATTAAAAGAAAAGACGAGGCGAAGTGG
IRF7	TCCCAGACTGCCTGTGTAGACGGAG	GAACTATTTATTGGGAGTTGGGATT
IRF9	TGTTGCCTCTGTAGATGCTTGGGAG	CCGACCAAGAGTGTGGAGAACAAGTC
ADAR	GCACTATGTCTCAAGGGTTCAGGG	GGTAGGGCTGTAGAAGGAGGGC
TRIM30	ATGGCCTCATCAGTCCTGGAGATGATAAAG	TTAGGAGGGTGGCCCGCATATAGTCATTGG
TRIM34	ATGGCCTCAACAGGTCTGACGAATATACAG	TCAGGAGTTCAGAGGACACAGGGTCATGGG
STAT1	TGGGAACGGAAGCATTTGGAATC	TGGGAAAAAAATGTCGCCAGAGAG
IFIT3	CATGAGTGAGGTCAACCGGGAA	CTATGTTTGCTCTTTAACCTCTTC
TNFα	TCCCAGAAAAGCAAGCAGCCAAC	AGTTCAGTAGACAGAAGAGCGTGG
IL-6	CAAAGCCAGAGTCCTTCAGAGAGATACAG	TGGATGGTCTTGGTCCTTAGCCAC

Table 2: **Primers used in RT-PCR.**

Electrophoretic Mobility Shift Assays

EMSAs were conducted on cell lysates obtained using lysis buffer made from 1% Nonidet P-40, 50 mM Tris (at a pH of 7.4), 150 mM NaCl, 30 mM NaF, 5 mM EDTA, 10% glycerol, 40 mM β-glycerophosphate, 1 mM PMSF, and supplemented with 5 μg/mL each of leupeptin, pepstatin, and aprotinin. Following incubation of cells for 20 minutes in 4 C, cell lysate suspensions were centrifuged to remove the membrane component. The supernatant was then quantified by Bradford Assay (Biorad) according to the distributor's instructions. 2-8 μg of protein equilibrated in buffer with 10 mM HEPES (pH 7.9), 2% glycerol, 40 mM KCl, 1 mM EDTA, 0.2 mM $MgCl_2$, and 1 mM DTT were incubated on ice with 1 μg poly-dIdC for ten minutes before incubation with radiolabeled probe.

Probes were purchased in single-stranded form and slow-annealed with their reverse complement at room temperature following boiling. Annealed probes were labelled with T4 Polynucleotide Kinase (New England Biolabs) using γ^{32}P-ATP. Probe incubation occurred for twenty minutes at room temperature. Supershift analysis was performed with the incubation of antibody with protein and poly-dIdC on ice for

Probe	Sequence: 5' to 3'
ADAR ISRE	CGGGGAAGCCTTTTCAAGGAAACGAAAGTGAACTC
TRIM30-417	ACTTGAAACACAAACTAGACA
TRIM30-1371	AACTGAGAAAAAGAAACTAAAGAACTAC
TRIM30-7648	GGGACACAGTGAAACTAACAG
TRIM30-9838	CAGAGTAGATGAAACTCTGAA
TRIM34-867	TATGAAAATAGAATCTGCAGC
TRIM34-1384	AGAGAAAAGAAACTGAAACTCCAAACCA
TRIM34-1393	GCAGAGAAAAGAAACTGAAAC
TRIM34-3818	GTCAGTCCTGTTTACCCTTTCAAAGGAC
TRIM34-4358	GTTCCTTTTGCCTTCTCTTTCCTGTGCC
TRIM34-4248	GACGAAAAGTGAGACTTGGTC

Table 3: **Probes used in EMSA.**

thirty minutes. C/EBPα antibody was employed as a control antibody. Samples were resolved on a 7% native gel composed of 49:1 Acrylamide:bis-acrylamide in a 0.5$\times$ TBE based buffer. Gels were dried and exposed by autoradiogram. Probe sequences are listed in Table 3. Numbers next to the probe name refer to the distance of the sequence from the point 1500 base pairs upstream of the transcriptional start site.

Affymetrix Analysis

cDNA from total RNA extracted from cells was created and subjected to analysis by Affymetrix microarray (Mouse Whole Genome Array 430 2.0). Known ISGs were accompanied by either a ten-fold or higher increase in transcriptional levels or a switch in status from negligible transcriptional levels (as defined by a raw expression score of 300 or lower) to significant in wild type MEFs treated with IFN. Genes were noted which showed a significant change in inducibility between wild type MEFs and IKKε deficient MEFs (as defined by the ratio of expression between IFN-stimulated sample and unstimulated sample).

Western Blot

Cell lysates were obtained using Nonidet P-40 lysis as described above. Proteins were mixed with buffer to give final concentration of 75 mM Tris (pH 6.8), 0.6% SDS, 15% glycerol, and 7.5% β-mercaptoethanol stained with 0.001% bromophenol blue. Samples were run on an 0.001% SDS, 10% 29:1 Acrylamide:bis-acrylamide gel with a running buffer consisting of 0.001% SDS, 0.003% Tris, 0.014% Glycine at a constant 55 mA using Biorad Precision Plus Protein Standards. Proteins were then transferred onto nitrocellulose membrane overnight at constant 20 V at 4 C using transfer buffer consisting of 20% methanol, 1.6% Glycine, and 0.003% Tris base.

Following transfer, the nitrocellulose membrane was blocked for a minimum of one hour in 5% milk in 5% Tween-20 in PBS. Antibody dilutions were also made in 5% milk solution and antibody incubations were done for one hour at room temperature. Primary antibody against GFP was made at 1 μg/mL. In between incubations, the blot was washed a minimum of 5 times for 5 minutes in 5% Tween-20 in PBS. Blots were visualized by incubation with ECL HRP-conjugated secondary antibodies (GE Healthcare) against Mouse IgG and Rabbit IgG depending on primary antibody used at a 1:5000 dilution of the manufacturer's stock. Immobilon Western HRP Substrate and Luminol reagent (Millipore) were used as the substrate for HRP.

Cloning

TRIM30 and TRIM34 GFP fusion constructs were made using Invitrogen's Gateway system. TRIM30 and TRIM34 were cloned from cDNA as described above with a cycle count of 30. PCR products were ligated into pCR 4-TOPO using Invitrogen's Topo TA Cloning Kit as per manufacturer's instructions. Resultant plasmids were amplified by bacteria. Attb-PCR products were then made using the primers listed in Table 4 at a cycle count of 30. PCR products were then gel-purified using Qiagen's QIAquick Purification Kit. PCR products were then used in the Gateway system with

Primer	Sequence: 5' to 3'
TRIM30-attl F	GGGGACAAGTTTGTACAAAAAAGCAGGCTTCATGGCCTCATCAGTCCTGGA
TRIM30-attl R	GGGGACCACTTTGTACAAGAAAGCTGGGTCTTAGGAGGGTGGCCCGCATATAGT
TRIM34-attl F	GGGGACAAGTTTGTACAAAAAAGCAGGCTTCATGGCCTCAACAGGTCTGACG
TRIM34-attl R	GGGGACCACTTTGTACAAGAAAGCTGGGTCTCAGGAGTTCAGAGGACACAG

Table 4: **Primers used for Gateway cloning**.

pDONR-Zeo as the donor vector and pDest-53 as the GFP-containing destination vector as per manufacturer's instructions.

Plaque Assay

VERO cells at hyperconfluent density in six-well plates were used for plaque assay. Log dilutions of virus stock from the collected media 9 hours following IFN stimulation or VSV infection were added to each well. Following incubation at 37 C for one hour, media was removed and replaced with 1% methylcellulose and left untouched for three days, after which VERO cells were fixed with 4% formaldehyde for a minimum of one hour and then stained with 0.2% crystal violent solution (in 20% ethanol) for 5 minutes. Crystal violet solution was washed off in water until plaques became visible.

Results

TRIM30 and TRIM34 Expression

tenOever et al recently published a study employing Affymetrix analysis of wild-type and IKKε deficient mouse primary fibroblasts both untreated and treated with IFNβ for 6 hours to study the role of IKKε (*31*). Expression levels of ISGs showed a difference in IFNβ induction between wild-type and IKKε deficient cells. A broad summary of ISG expression in the absence of IKKε is shown in Figure 3.

TRIM30 and TRIM34 are two genes which were shown by Affymetrix analysis to be significantly dependent on IKKε for proper Type 1 IFN-induction. To recapitulate

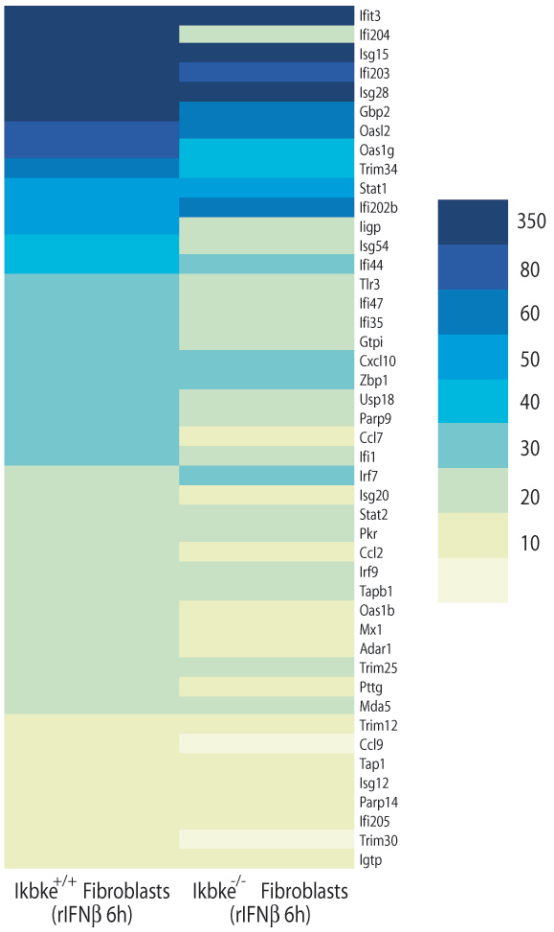

Figure 3: **A subset of ISGs show loss of Type 1 IFN-induction in IKKε deficient cells.** Affymetrix analysis was conducted on cDNA made with extracted RNA from IKKε +/+ and -/- cells untreated or treated with recombinant IFNβ for 6 hours. Heat map depicts mean IFN-induction among replicates. (Figure from tenOever et al (*31*))

this *in silico* phenotype, cDNA was prepared using RNA harvested from IKKε wild type and knockout mouse embryonic fibroblasts (MEFs) treated with recombinant IFNβ for 0 hours, 3 hours, and 6 hours. This was then subjected to RT-PCR to check for expression levels of TRIM30 and TRIM34 (Figure 4). As expected, IFNβ treatment in wild type cells upregulated a full range of ISGs in a time-dependent manner (Figure 4, lanes 1-3), but not non-ISGs such as IFNβ. Additionally, in cells lacking IKKε, while ISGs like IRF7 showed proper induction, ISGs such as ADAR, TRIM30, and TRIM34 showed severely compromised activation in response to IFNβ treatment (Figure 4, lanes 4-6).

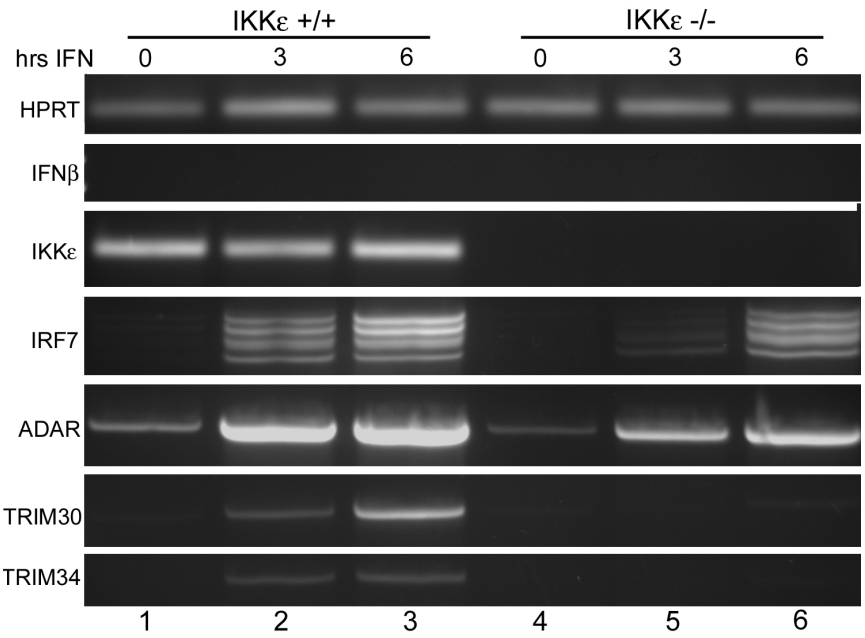

Figure 4: **TRIM30 and TRIM34 expression requires IKKε.** RT-PCR analysis was conducted on RNA harvested from IKKε +/+ (lanes 1-3) and -/- cells (lanes 4-6) untreated (lanes 1 and 4) or treated with recombinant IFNβ for 3 (lanes 2 and 5) or 6 hours (lanes 3 and 6).

TRIM30 and TRIM34 Gene Structure

TRIM30 and TRIM34 are members of the Tripartite Motif family of proteins. Microarray probes corresponding to the IFN-induction phenotype described above were tracked to specific accession numbers from the NCBI Entrez Nucleotide (`http://www.ncbi.nlm.nih.gov/entrez/query.fcgi?db=Nucleotide`) and was confirmed by RT-PCR with primers flanking the cDNA of the genes (Figure 4). Through UC Santa Cruz's Genome Bioinformatics Mouse BLAT search (`http://genome.ucsc.edu/cgi-bin/hgBlat`) and NCBI Entrez Protein (`http://www.ncbi.nlm.nih.gov/entrez/query.fcgi?db=Protein`), the genetic and protein structures of TRIM30 and TRIM34 were determined (Figure 5). Both genes are located on mouse Chromosome 7 which is also the location of several other TRIM proteins: TRIM12, TRIM21, TRIM6, TRIM68, and TRIM72. While human cells do not have a version of TRIM30, the human orthologs to almost all of these genes (in-

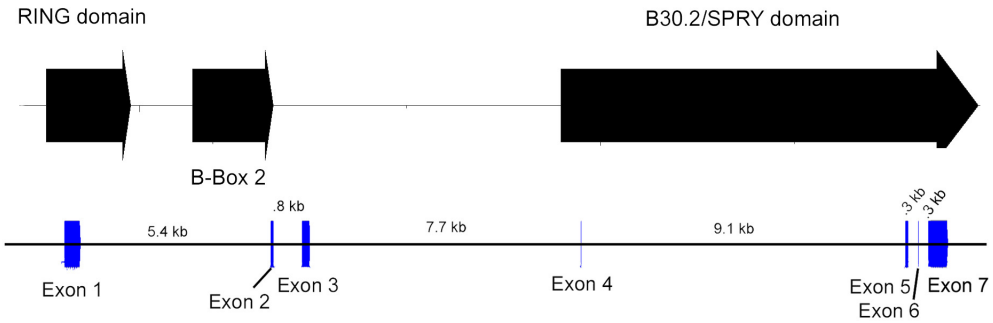

(a) TRIM30 (cDNA: NM009099.2, protein: NP033125.2, 496 amino acids, 57.3 kDa)

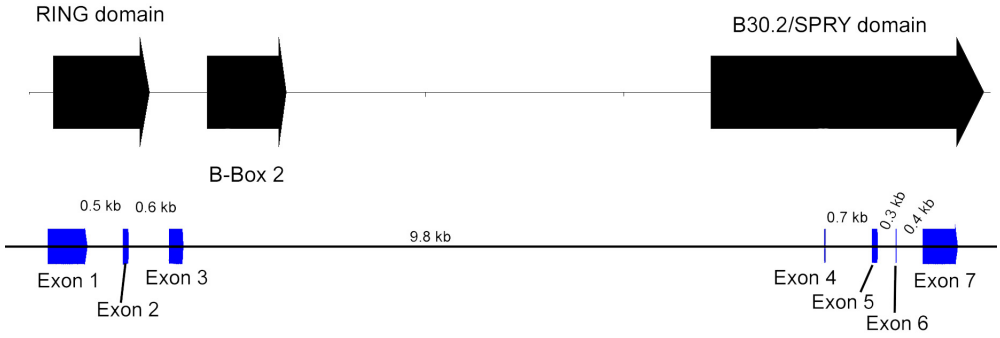

(b) TRIM34 (cDNA: AF220139, protein: AAG53512.1, 485 amino acids, 55.9 kDa)

Figure 5: **TRIM30 and TRIM34 genetic and protein structure.**

cluding TRIM34) are found on human Chromosome 11. Bioinformatics databases also show that both TRIM30 and TRIM34 have several reported splice variants (TRIM30 has 1, TRIM34 has 3), all of which encode much shorter proteins than the ones predicted by the accession numbers in Figure 5, although no specific biological function has been ascribed to any.

TRIM30 and TRIM34 Functional Characterization

Preliminary functional studies conducted on TRIM30 and TRIM34 suggested the proteins as possessing antiviral properties tied to innate immunity. Nan Zhu's preliminary studies on TRIM34 revealed that the virus titer in cell media from MEFs transfected with TRIM34 is lower than in cell media from cells transfected with a control plasmid (personal communication). Analogous studies with TRIM30 (Figure 6) demonstrated that cells overexpressing a TRIM30 construct activate IFNβ and a

wide range of ISGs (Figure 6a), increased ISGF3 binding to ISREs (Figure 6b, lane 4 compared with lane 3), and reduced viral titer in the media (Figure 6c). Although the specific mechanisms by which these occurred were not elucidated, they did suggest a role for the two proteins in antiviral defense. Splice variations in these original constructs, however, caused translated products to be consistently truncated, possibly explaining the inability to visualize them by Western blot, but sequence analysis demonstrated that the RBCC motifs in these constructs were not affected, implying that the antiviral properties of TRIM30 and TRIM34, and quite possibly other TRIMs, can be attributed to that functional domain.

To more accurately test the functions of TRIM30 and TRIM34, plasmids encoding N-terminal GFP-tagged versions of TRIM30 and TRIM34 as predicted by the Microarray data were constructed using Invitrogen's Gateway system. These constructs were then transfected into MEFs and visualized under fluorescence microscopy (Figure 7a). Fluorescence microscopy revealed a diffuse cytoplasmic localization with a slightly higher concentration closer to the nucleus for TRIM30 and cytoplasmic patches for TRIM34. These cells were subsequently lysed and subjected to Western Blot with anti-GFP showing both TRIM30 (Figure 7b [left] lane 2, [right] lane 2) and TRIM34 (Figure 7b [right] lane 3) protein migration under 75 kDa, a molecular weight lower than the expected molecular weight of a TRIM30-GFP fusion (57 kDa + 25 kDa = 82 kDa) or a TRIM34-GFP fusion protein (56 kDa + 25 kDa = 81 kDa). This interesting observation was accompanied by the fact that higher exposure times on TRIM30 blots showed the presence of proteins migrating faster than the main band and in TRIM34 blots, a faint and migrating higher than the main TRIM34 band was also visible, suggesting the possibility of TRIM30 and TRIM34 processing.

The potential immunological function of TRIM30 was investigated by infecting MEFs transfected with GFP-TRIM30 with Sendai Virus. These cells were visualized under fluorescence microscopy to see localization changes in response to immunologi-

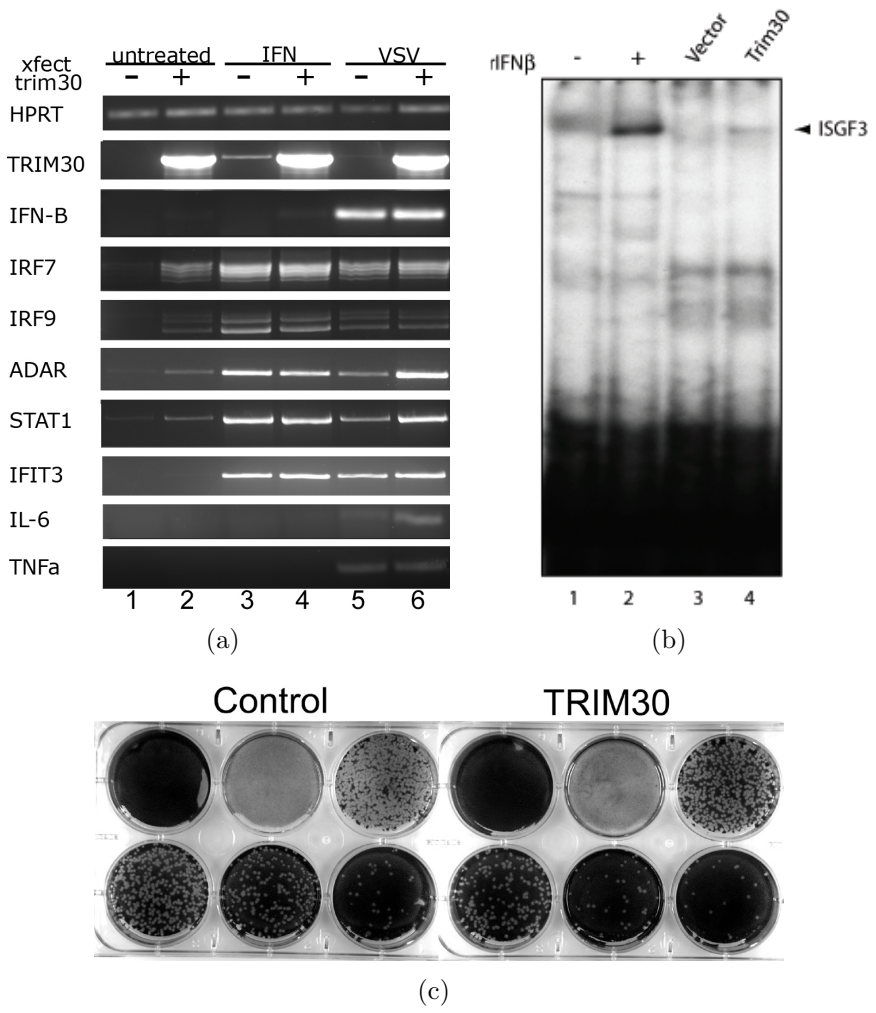

Figure 6: **TRIM30 is a component of the antiviral response.** *(a)* RT-PCR was performed on RNA extracted from MEFs transfected with TRIM30 and with a control plasmid. *(b)* Whole cell lysate was run on a gel shift assay using the ISRE of oligoadenylate synthase (OAS), an IFN-stimulated gene as the probe. Cell lysate from MEFs untreated and treated with IFNβ is shown as a positive control. *(c)* Plaque assays were performed on media collected from VSV-infected MEFs transfected with TRIM30 (right) and with a control plasmid (left). Replicates in 6 well plates represent log-dilutions of virus and the upper-left well in both plates represents a no virus control.

cal stimuli (Figure 7c), revealing that viral infection concentrates TRIM30 to specific cytoplasmic pockets. This finding suggests that TRIM30 is either recruited or post-translationally modified following viral infection and is a possible clue to its function.

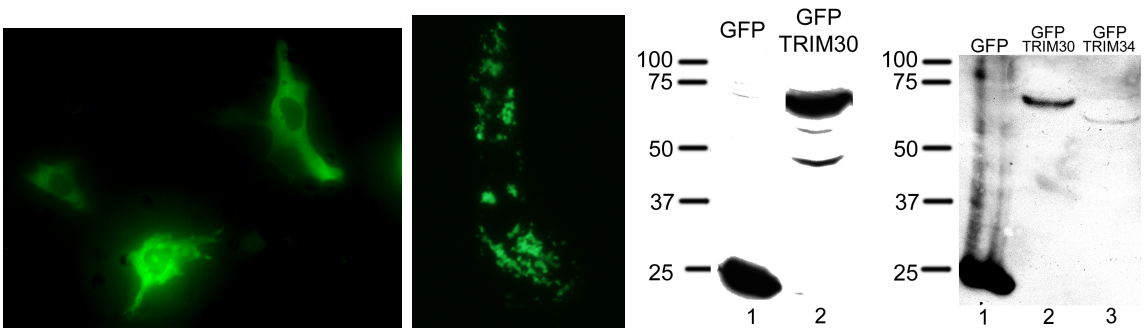

(a) GFP-TRIM30 (b) GFP-TRIM34 (c) WB: anti-GFP

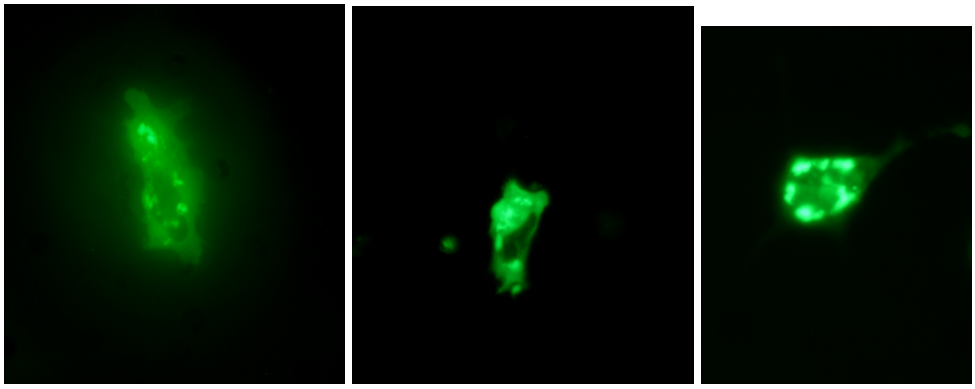

(d) GFP-TRIM30 + Sendai Virus (left,middle) and MAVS (right)

Figure 7: **TRIM30 responds to viral infection.** MEFs were transfected with GFP-TRIM30 *(a)* and GFP-TRIM34 *(b)* constructs and viewed under fluorescence microscopy at 640×. *(b)* Whole cell lysates of cells from *(a)* and *(b)* were run on Western blot *(c)* and probed with anti-GFP with lysate from cells transfected with GFP only (26 kDa) as a positive control (left, lane 1; right, lane 1). A higher exposure with TRIM30 only is also shown (left). *(d)* MEFs transfected with GFP-TRIM30 were infected with Sendai Virus (left, middle) and co-transfected with MAVS (right). GFP-TRIM30 localization was visualized under fluorescence microscope at 640×.

TRIM30 and TRIM34 Transcriptional Regulation

Components of the innate immune system require tightly regulated and functionally-specific transcriptional control. To determine the transcriptional control element responsible for TRIM30 and TRIM34's transcriptional regulation, the genomic sequences for TRIM30 and TRIM34 were obtained from UCSC's BLAT. All DNA from the start codon of the genes to 1500 base pairs upstream of the transcriptional start site were analyzed with the transcription binding site finder Matinspector. All transcriptional binding sites labelled by Matinspector as an IRF7 binding site, an IRF3

Figure 8: **The consensus sequence for an ISRE is GAAANNGAAACNN(A/T).** Known ISREs were aligned and a consensus sequence for the critical residues (outlined in black) was created. (Figure from tenOever et al (*31*))

binding site, or an ISRE were recorded and reasonably close matches to the consensus sequence of ISRE (GAAANNGAAACNN[A/T], see Figure 8) were isolated and made into probes for EMSA (see Materials and Methods for list of probes).

Probes were first tested for IFN-inducibility. Wild-type MEFs were either mock-treated or treated with IFNβ and then lysed after six hours. These lysates were then tested on all probes for IFN-inducible binding (Figure 9) using the ADAR ISRE as a positive control (Figure 9, lanes 1-2). This initial screen resulted in the isolation of two probes, one for TRIM30 (TRIM30-1371, Figure 9, lanes 3-4) and one for TRIM34 (TRIM34-1384, Figure 9, lanes 5-6), which showed strong binding contingent on IFNβ treatment.

This IFN-induced binding was tested for IKKε dependence. Wild-type MEFs and IKKε knockout MEFs were either mock-treated or treated with IFNβ for six hours. EMSAs using these lysates and the TRIM30 and TRIM34 probes revealed weaker induced binding in cells deficient in IKKε (Figure 10a, lanes 4, 8, and 12 as compared with lanes 2, 6, and 10). Thus, the ISREs coded for in the probes mirrored the induction patterns of the genes in question.

The identity of the complex binding the ISRE sequence was tested by super-shift assay, employing antibodies to disrupt or increase the molecular weight of the DNA:protein complex (Figure 10b). While a control antibody (anti-C/EBPα) failed to affect the binding at the probe for both TRIM30 and TRIM34 (Figure 10b, lanes

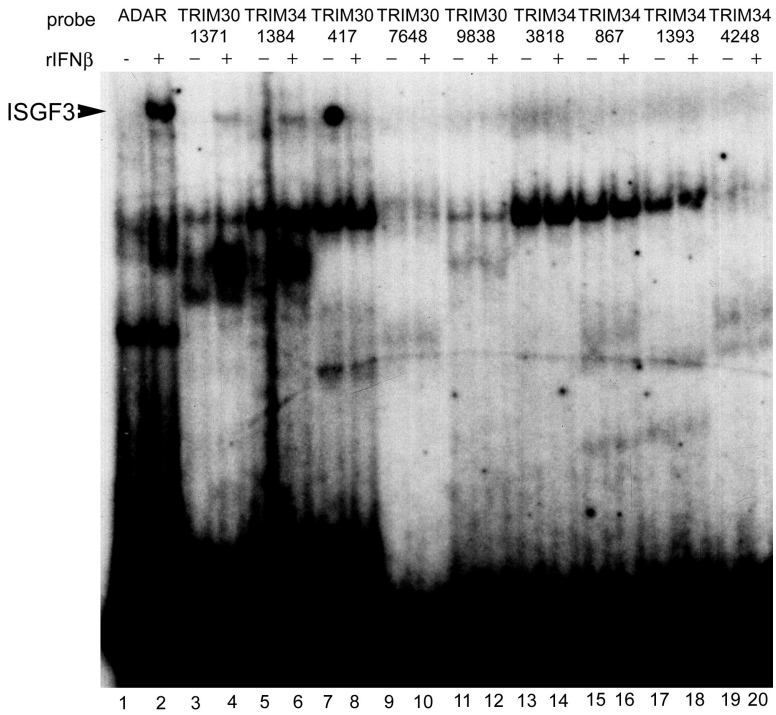

Figure 9: **ISREs from TRIM30 and TRIM34 enhancer are IFN-inducible.** Probes were created by searching the genomic DNA from 1500 base pairs upstream of the transcriptional start site until the start codon. Radiolabeled probes were incubated with cell lysates from wild-type MEFs mock-treated and treated with IFNβ for 6 hours and then run on gel shift assay. Numbers next to the probe name refer to the distance of the sequence from the point 1500 base pairs upstream of the transcriptional start site.

3 and 8), an antibody to STAT1α reduced binding (Figure 10b, lanes 4 and 9) and an antibody to STAT2 shifted the complex upwards (Figure 10b, lanes 5 and 10), showing that the complex binding to the ISRE is most likely ISGF3 which consists of both STAT1 and STAT2.

Viral Transcriptional Regulation

In general, ISGs can be activated by both stimulation with IFNβ and infection by virus. However, because infection by virus leads directly to the production of IFNβ, it is difficult to separate the effects of the two transcriptional inducers. To investigate the possibility of a direct viral induction independent of IFN of TRIM30 and TRIM34, gene expression after immunological stimulation of Sv129 MEFs, which encode an

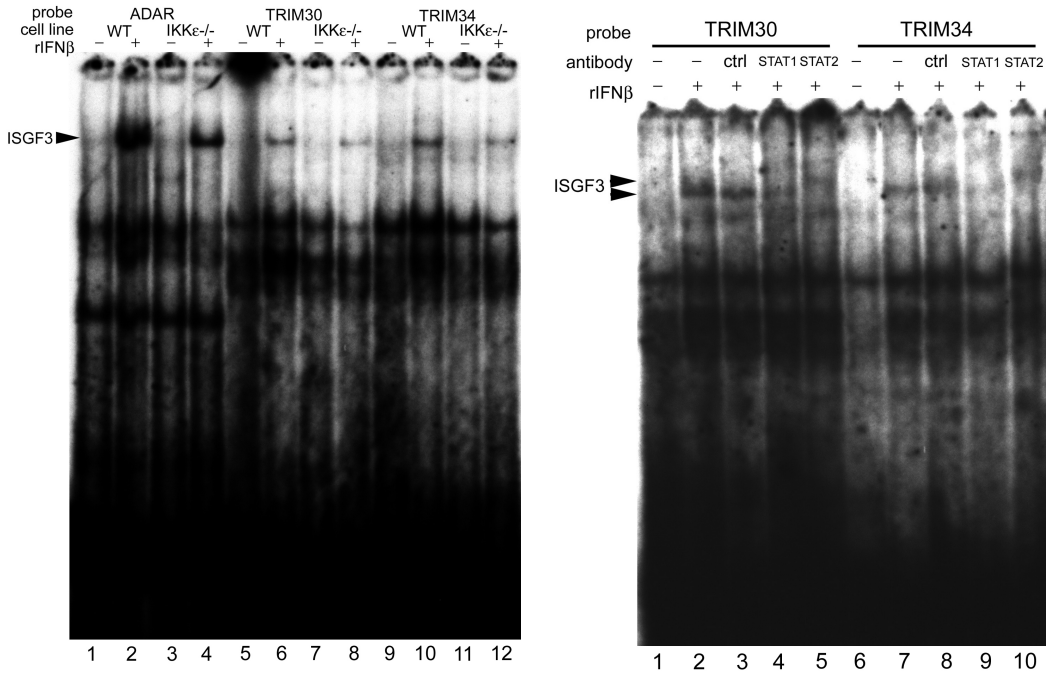

(a) IKKε Dependent Binding (b) ISGF3 Supershift Assay

Figure 10: **ISREs from TRIM30 and TRIM34 bind ISGF3 in an IKKε dependent manner.** Cell lysates from wild-type and IKKε deficient MEFs were mock-treated or treated with recombinant IFNβ for six hours were incubated with radiolabeled probes containing TRIM30 and TRIM34 ISRE and run on gel shift assay *(a)* to assay the difference in IFN-induced TRIM30/TRIM34 ISRE binding between wild-type and IKKε knockout cells and *(b)* as part of a supershift assay with the antibodies listed to identify the complex binding at the ISRE. An antibody to C/EBPα was employed as a supershift negative control antibody.

IFNAR1 with a disruption in exon 3 rendering it inactive by frameshift mutation, was compared with the expression profile of stimulated wild-type MEFs. As viruses engage in many forms of IFN production and signaling antagonism (*3*), double stranded RNA (dsRNA) was used to avoid viral antagonism pathways to produce a stronger signal. RT-PCR was conducted on RNA extracted from mock-stimulated, six hour IFNβ stimulated, or six hour dsRNA treated Sv129 and wild-type MEFs (Figure 11). RT-PCR analysis shows that while viral replication intermediates were perfectly able to induce IFNβ in cells lacking functional IFNAR1, it was unable to upregulate levels of ADAR, TRIM30, and TRIM34, suggesting that their transcriptional control in MEFs was mediated primarily through IFNβ production (Figure 11, lanes 3 and 6).

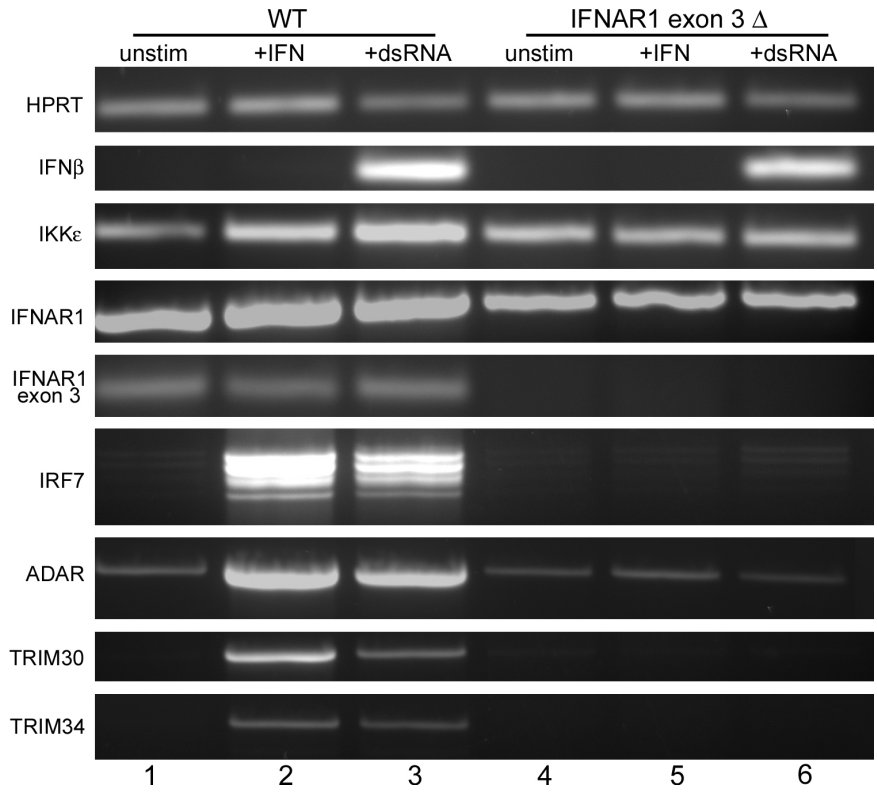

Figure 11: **TRIM30 and TRIM34 expression in cells with nonfunctional IFNAR1.** RT-PCR analysis was conducted on RNA harvested from wild-type (lanes 1-3) and Sv129 (IFNAR1 exon 3 disruption) cells (lanes 4-6) untreated (lanes 1 and 4), treated with recombinant IFNβ for six hours (lanes 2 and 5), and transfected with double-stranded RNA for six hours (lanes 3 and 6).

Employing the fact that an ISRE can also bind IRF family proteins such as IRF3 and IRF7 which are activated by viral infection, this phenotype was explored by bandshift assay (Figure 12). Protein lysates from wild-type and Sv129 cells mock-treated, treated with IFNβ for six hours, or transfected with dsRNA for six hours were incubated with the probes containing the ADAR (Figure 12a), TRIM30 (Figure 12b), and TRIM34 ISRE (Figure 12c). The bandshifts reveal that the inability to induce the three genes in Sv129 cells most likely stems from a lack of binding to the ISRE (Figure 12a-c, lanes 4-6 as compared with lanes 1-3).

Interestingly, an induction of IRF7 was observed in dsRNA-transfected Sv129 cells (Figure 11, lane 6), suggesting that IRF7 is a gene which can be directly induced by virus. This is of particular note as it is known that viral infection leads to the

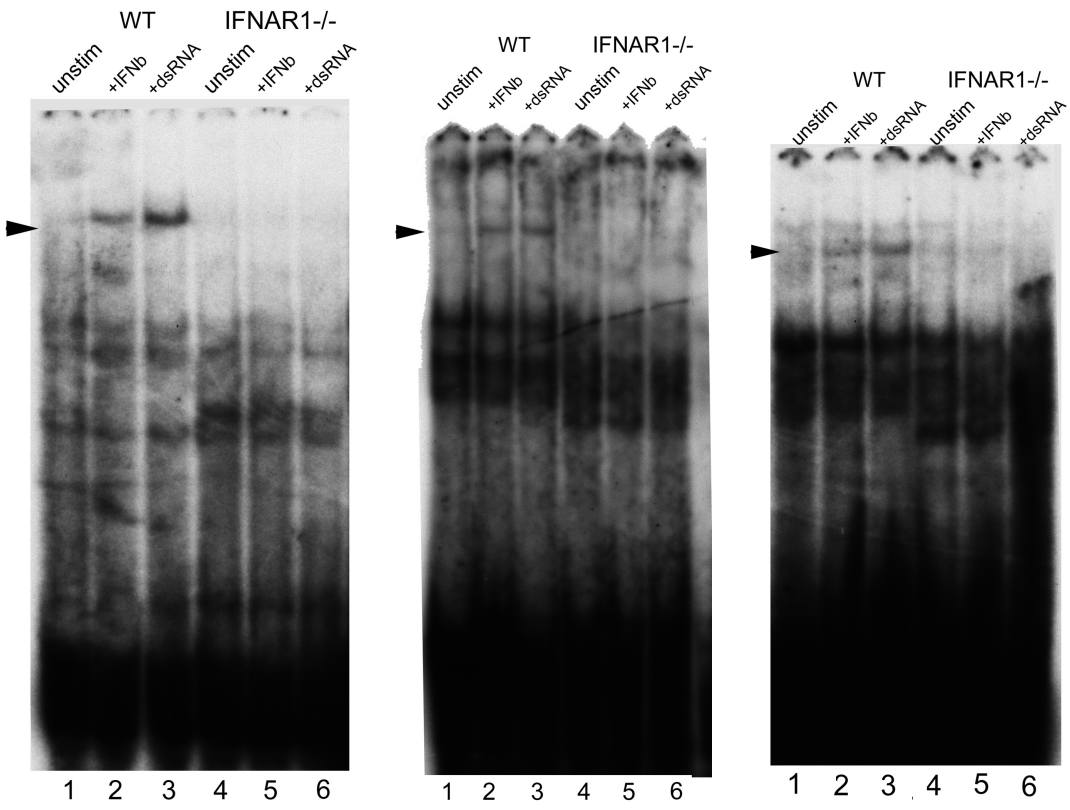

(a) ADAR ISRE (b) TRIM30 ISRE (c) TRIM34 ISRE

Figure 12: **TRIM30 and TRIM34 ISREs are not bound in absence of IFN signaling.** Wild-type and Sv129 cells mock-treated (lanes 1 and 4), treated with IFNβ for six hours (lanes 2 and 5), and transfected with dsRNA for six hours (lanes 3 and 6) were incubated with the ISREs of *(a)* ADAR, *(b)* TRIM30, and *(c)* TRIM34.

phosphorylation of IRF7 and IRF3, a phenomena which has been used to explore the distinction between Type 1 IFN-regulated genes and viral-stimulated genes (*52*). As basal IRF7 levels are low in most cell types, it is possible that the lack of IFN-independent viral induction of genes in a fibroblast cell line was due to a low level of IRF7 and the inability of IFNβ production to upregulate IRF7. To investigate the possibility that cells expressing high basal levels of IRF7 (i.e. APCs and other leukocyte lineages) could bind the ISRE of TRIM30 and TRIM34, cell lysates of MEFs transfected with plasmids containing FLAG-tagged IRF7 and IKKε (which phosphorylates IRF7) were incubated with the ADAR, TRIM30, and TRIM34 ISREs and assayed by supershift (Figure 13). TRIM30 (Figure 13b) showed a complete

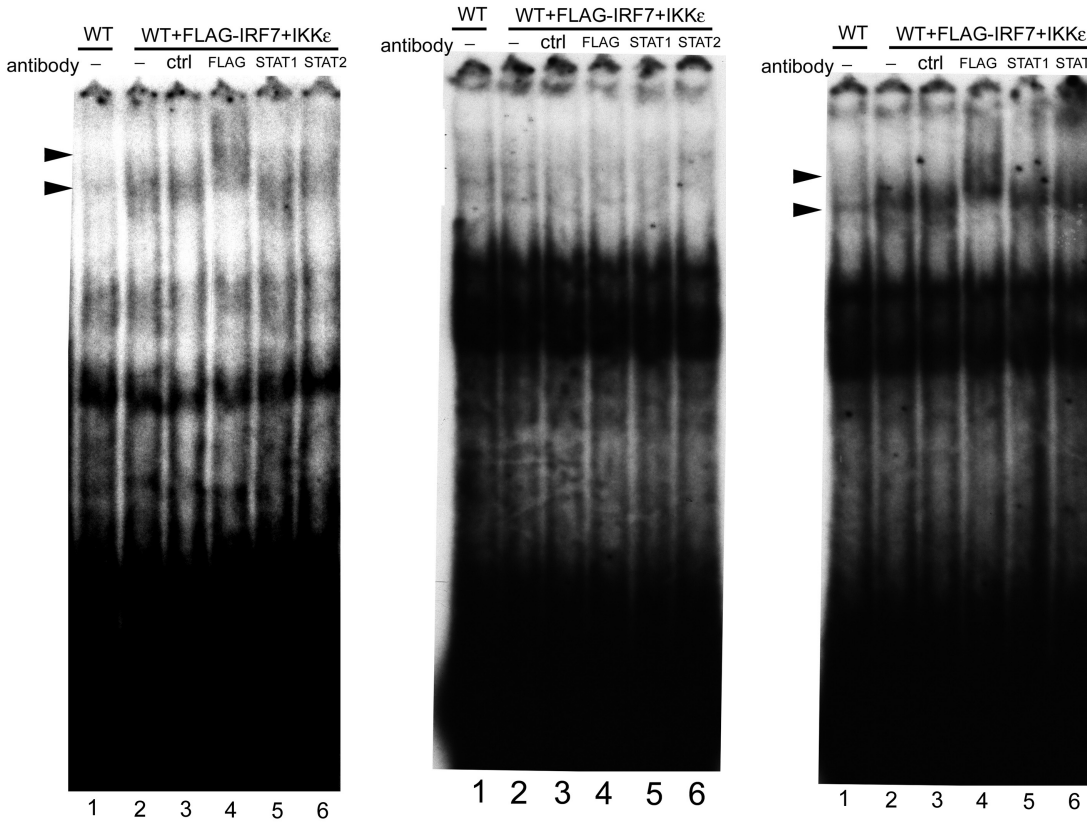

(a) ADAR ISRE (b) TRIM30 ISRE (c) TRIM34 ISRE

Figure 13: **ADAR and TRIM34 ISREs can bind IRF7.** Wild type MEFs (lane 1) and MEFs overexpressing IKKε and IRF7 (lanes 2-6) were lysed and used to perform supershift assays with ISREs for *(a)* ADAR, *(b)* TRIM30, and *(c)* TRIM34 with the antibodies listed. An antibody against C/EBPα was employed as an antibody control.

lack of binding, implying that its induction is completely IRF7 (and hence virus) independent. TRIM34 (Figure 13c) and ADAR (Figure 13a), however, showed a large protein complex binding at the ISRE (Figure 13a and 13c, lane 2). While control antibody and STAT1 and STAT2 antibodies failed to shift or disrupt the complex (Figure 13a and 13c lanes 3, 5, and 6), an anti-FLAG antibody shifted the complex (Figure 13a and 13c, lane 4), suggesting that cells expressing high levels of IRF7 may indeed bind the ISRE in an IFN-independent manner.

This hypothesis was tested in the case of the ADAR ISRE by performing supershift assays on lysates from macrophages, a cell type expressing high levels of IRF7, treated with IFNβ (Figure 14 lanes 2-5), or infected them with Influenza Virus (WSN1 strain)

(Figure 14, lanes 6-9). In IFNβ treated macrophages, while the control antibody does not affect the complex binding the ISRE (Figure 14, lane 3), STAT1 antibody weakens the complex (Figure 14, lane 4) and STAT2 antibody abrogates it entirely (Figure 14, lane 5), suggesting that the complex is ISGF3 or some other STAT2-driven complex. In WSN1 treated macrophages, neither STAT1 nor STAT2 antibody completely abrogate binding (Figure 14, lanes 8 and 9), although they dramatically weaken the complex. The difference in the supershift profiles implies a difference in the composition of the complexes binding at the ISRE when stimulated directly with IFNβ and with virus. The significant loss in binding notes that even in cells with high basal levels of IRF7, the dominant factor controlling transcription of genes like ADAR and TRIM34 is ISGF3. However, the persistence of binding coupled with the data showing that IRF7 can bind to these elements suggests that IRF7 does play a role in the transcriptional upregulation of these genes.

Discussion

The Role of TRIM Proteins in Innate Immunity

The data here presents preliminary evidence that TRIM30 and TRIM34 are members of the rapidly expanding family of TRIM proteins with immunological roles (refer to Table 1). TRIM30 and TRIM34 constructs were demonstrated to restrict viral titer and upregulate a series of ISGs (Figure 6). Through fluorescence imaging, the localization of TRIM30 was found to be altered by viral infection and by co-transfection with MAVS, a stimulator of innate immunity pathways, suggesting that TRIM30 is either recruited and/or processed in response to an immunological stimulus (Figure 7). The pattern of TRIM34 localization also appears to be similar to the localization of the viral-stimulated TRIM30. This, coupled with the fact that TRIM30 and TRIM34 are ISGs which require IKKε (which has been shown to control the upregulation of a

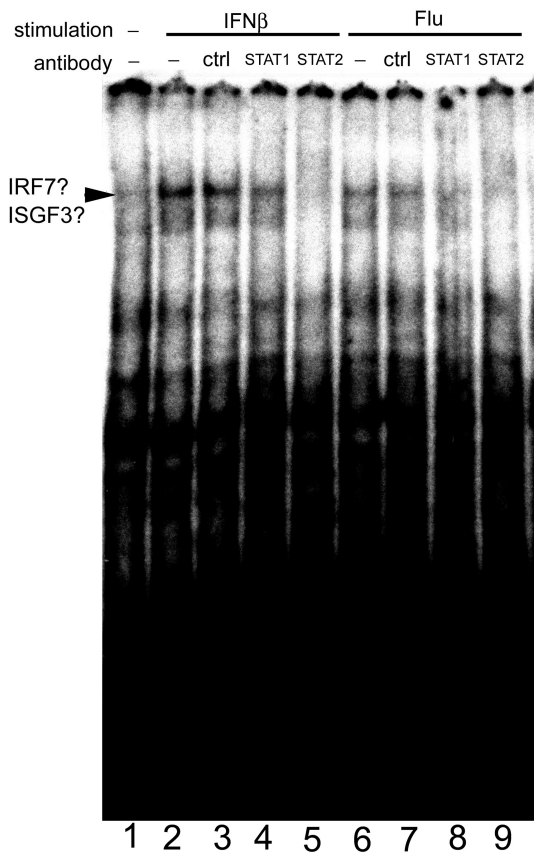

Figure 14: **Macrophages show IRF7 binding at the ISRE.** Cell lysates from macrophages mock-treated, treated with IFNβ (lanes 2-5), or infected with WSN1 (lanes 6-9) were run on a supershift assay with the ADAR ISRE using the antibodies listed. An antibody against C/EBPα was employed as an antibody control.

set of genes critical to the host innate response to viral infection) to properly induce, strongly suggests that these two proteins play an important role in innate immunity.

While the precise mechanisms of action for TRIM30 and TRIM34 remain to be elucidated, this study presents some promising observations with regards to how TRIM30 and TRIM34 may act. Western blot shows that TRIM30-GFP and TRIM34-GFP fusion proteins migrate at a lower molecular weight than one would expect (Figure 7). This was accompanied by the fact that protein bands migrating at still lower molecular weights could be seen at higher exposure times for cells transfected with TRIM30, suggesting that TRIM30 and TRIM34 processing are functionally relevant.

This is unsurprising given that the literature suggests strongly that the tripartite motif in TRIM proteins mediates E3 ubiquitin ligase activity, an activity which is oftentimes associated with the E3 ligase mediating auto-ubiquitination and subsequent proteolytic processing. Ubiquitination as a means of innate immune pathway regulation has already been demonstrated to be of widespread and critical importance as demonstrated by the fact that proper NF-κB activation requires ubiquitination (*39*). This occurs on several levels: on the level of the ubiquitin-mediated regulation of upstream mediators of NF-κB such as TRAF2 and TRAF6, on the level of the processing of the NF-κB p100 precursor to its active form p50, and on the level of the degradation of the NF-κB inhibitor IκB following its phosphorylation by the canonical IKK kinases. The role of TRIMs in ubiquitin-mediated innate immunity control is also not unprecedented as shown by the recently published role of TRIM25 in the ubiquitination of RIG-I.

Subsequent studies will focus on clarifying the functional roles of TRIM30 and TRIM34. A broad gene expression analysis on cells overexpressing TRIM30 and TRIM34 can help clarify if and how the proteins mediate their antiviral functions through transcriptional regulation, as suggested by preliminary studies (Figure 6). These can be followed up by bandshift assays to ascertain the specific components responsible for any potential transcriptional regulatory differences induced by the TRIM proteins.

TRIM30 and TRIM34 could also mediate its effects on proteins post-transcriptionally, at the level of translational control or by altering the broad pattern of post-translational modification or regulation (i.e. activating kinases or other E3 Ubiquitin Ligases). In either case, FLAG-tagged versions of TRIM30 and TRIM34 will be created for the purposes of Co-Immunoprecipitation assays and for Mass Spectrometry in order to identify and examine possible substrates and binding partners, in particular any E2 Ubiquitin-conjugating enzymes which may assist TRIM30 and TRIM34 in mediat-

ing ubiquitination. Cotransfection with TRIM30 or TRIM34 of a tagged-version of ubiquitin (i.e. HA-tagged) with a hypothetical substrate can also be used in HA-immunoprecipitation experiments to explore which substrates TRIM30 and TRIM34 ubiquitinate.

While the precise role of TRIM30 and TRIM34 remain to be determined, the abundance of preliminary evidence and the details pertaining to their transcriptional regulation strongly suggest an important role for these two proteins in mediating the antiviral state.

TRIM30 and TRIM34 Transcriptional Control

This study details gene regulation motifs of the antiviral system with regards to TRIM30 and TRIM34. The data here shows that TRIM30 and TRIM34 are ISGs which require functioning IKKε for proper transcriptional regulation (Figure 4). The genes are regulated by ISRE sequences in their promoter (marked in Table 3) which are bound strongly by ISGF3 in an IKKε dependent manner when the cell is stimulated with IFNβ (Figure 10). TRIM30 and TRIM34 are not upregulated significantly in the absence of Type 1 IFN signaling (Figure 11), suggesting that in most cell types it is ISGF3-mediated signaling which is the most important transcription factor involved in the transcriptional activation of TRIM30 and TRIM34.

It was possible, however, to show that IRF7, a major transcription factor involved in viral infection-induced signaling pathways, was capable of binding in a high molecular weight complex to the TRIM34 and ADAR ISRE sequences, but not the TRIM30 ISRE (Figure 13), thus suggesting that cell lineages which express high levels of IRF7, especially APCs such as macrophages and dendritic cells, may employ IRF7 as a means of regulating the expression of TRIM34 and other ISRE-controlled genes. Macrophages stimulated with IFNβ and virus indeed showed a difference in the transcription factor binding of the ADAR ISRE (Figure 14). This difference in

composition suggests that in APCs such as macrophages, detection of viral infection induces IRF7-controlled transcriptional upregulation of genes normally controlled by IFN signaling through ISGF3. However, the relatively low magnitude of this change still implies that IFN signaling plays the dominant role in the upregulation of genes activated by Type 1 IFN treatment.

These experiments, while preliminary, suggest multiple courses of future study with regards to the specifics of TRIM30 and TRIM34 gene regulation. To expand the analysis of IFN-independent viral-mediated transcriptional activation, it would be useful to transfect the IFNAR1 mutant cell line with FLAG-tagged IRF7 to note the ability of IRF7 in virus-infected or dsRNA-treated to bind the appropriate ISREs completely independently of IFN signaling. Gene expression analysis on these transfected Sv129 cells could also be used to determine the transcriptional impact and kinetics of IRF7 binding to those ISREs.

While supershifts demonstrate that IRF7 can indeed bind to the ISRE of TRIM34 and ADAR, it is not clear what other proteins are involved in the high molecular weight complex that binds the ISRE, a question which is puzzling as it has been reported that IRF7 on its own is unable to recruit the histone acetylase transcriptional coactivators CBP, p300, and PCAF (*53*). Given that the IRF7-containing complex which binds the ISRE runs at approximately the same molecular weight as ISGF3, a massive, trimeric complex also associated with the transcriptional coactivator CBP, it leads one to believe either that the report of IRF7's inability to bind transcriptional coactivators was wrong or that IRF7 binds a partner protein which can recruit this machinery. Additional supershift experiments involving purely endogenous proteins or involving overexpression of suspected binding partners will help elucidate the composition of this complex and possibly additional proteins and steps involved in this phenomena.

Of particular note is this study's confirmation of a published finding that IRF7

could be induced by viral stimulation independent of IFN signaling (*54*). IRF7 is considered a "master regulator" (*55*) of Type 1 IFN induction by virtue of its ability to bind a wide range of promoter sequences including the PRDs upstream of the IFNβ gene (*53*) and multiple ISRE sites (*54*). The weak induction of IRF7 by dsRNA in cells with abrogated IFN signaling thus implies that the timeline for the experiment, six hours, may not have been of sufficient duration to observe significant ADAR or TRIM34 activation due to lack of sufficient IRF7 upregulation, suggesting a longer kinetics experiment may be necessary to observe viral-mediated, IFN-independent activation.

While ISREs for TRIM30 and TRIM34 were found which show binding patterns on EMSA which recapitulate gene expression phenotypes, the sequences themselves have not been studied carefully except for postulated contact sites based on bioinformatics work and adopted crystal structure data. Interestingly, although each designed probe fit the ISRE consensus sequence with varying success, the probe sequences that show IFN-inducibility appear to fit the consensus site to the greatest degree. This, however, fails to explain the sharply different pattern of IRF7 binding between the functional ISRE sequences. Analysis of the ISRE sequences shows that the TRIM30 ISRE is a perfect consensus match while the TRIM34 ISRE is not, despite the fact that IRF7 bound only the TRIM34 probe. This suggests that the critical bases which determine IRF7 binding are outside the ISRE consensus. Further experiments will employ bandshift assays on TRIM30 and TRIM34 probes with introduced mutations to identify the source of this puzzling phenotype.

This study presents promising data pertaining to the transcriptional programming which regulates TRIM30 and TRIM34, two uncharacterized proteins implicated in innate immunity. The data presented explores the molecular basis of this transcriptional control and, with further kinetics and molecular analysis, may even suggest a functional role for the two TRIM proteins.

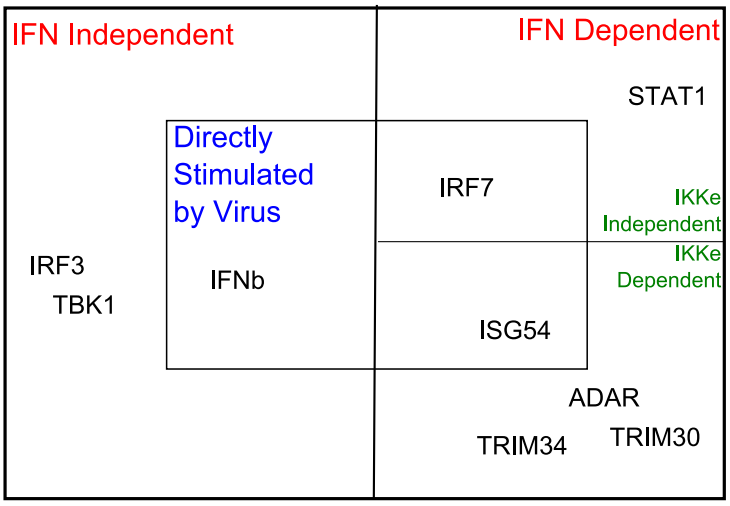

Figure 15: **ISG Characterization.**

Transcriptional Regulation in Antiviral Defense

The experiments here provide a prototype for a broader study of the wide range of genes known to play a role in mediating host defense against viral infection. From the current literature, one notes that such genes can be split into the categories listed in Figure 15. The most obvious divide in genes is between those which are stimulated by Type 1 IFN and those which are not. Of the genes that are Type 1 IFN-stimulated, two other overlapping classifications remain. The first is a divide between genes which can be upregulated directly by viral infection and those genes which can only be induced by IFN signaling. The second is a divide only recently published between ISGs which are dependent upon functioning IKKε and those which do not require IKKε to properly signal.

This complex gene network, coupled with the complex signal transduction pathways which regulate and are determined by this network, represents an intricate problem for complex systems analysis. However, because the links between components in biological networks are under constant evolutionary pressure from pathogens on the level of fairly easily modulated protein-protein and protein-DNA interactions (*56*), this complex system can best be understood from the context of performing its func-

tion — to quickly, effectively, and selectively coordinate a complex, multi-layered response.

This study looks at three major forms of transcriptional regulation employed by the host cell innate immunity: viral-activated IRF7 and IRF3, the mediator of IFN-signaling ISGF3, and the modulation of ISGF3 specificity through IKKε activity. While IRF7 is an ISG, its ability to be stimulated by viral infection without IKKε activity, to bind promiscuously at the IFNβ enhancer and at ISREs upstream of some ISGs suggests that IRF7 and its binding partner IRF3 mediate an immediate response to viral infection by stimulating the production of IFNβ and of certain ISGs. This immediacy is supported by the fact that IRF7 activation as a transcription factor is mediated directly by phosphorylation and does not require the synthesis or secretion of new proteins. Although slower to start, IFNβ production induces ISGF3 production in neighboring cells and in the producing cell. Supershift assays (Figure 14) and broad expression analyses (*52, 57*) show that ISGF3 is the dominant regulator of ISG induction. This is mediated most likely by a tight affinity between ISGF3 and transcriptional co-activators and the fact that the ISGF3 components are also ISGF3 targets.

This transcriptional circuit resembles two major biological network motifs. The first is an OR-gated Feed Forward Loop (Figure 16a,b) as either of the two input signals (IRF7 and IFNβ) is sufficient for gene induction of the genes which can both be stimulated directly by virus and by IFN. The properties of this particular network motif have been investigated significantly in sensory transduction networks (*56*). While they depend on the specific biological parameters of the transcription factors involved, they are generally conducive to a reduction in delay of activation of the genes in question, as only the early signal is needed for gene induction.

Because IFN signaling also acts to activate IRF7 through ISGF3 transcriptional activity and through activation of IKKε, the transcriptional circuit also resembles a

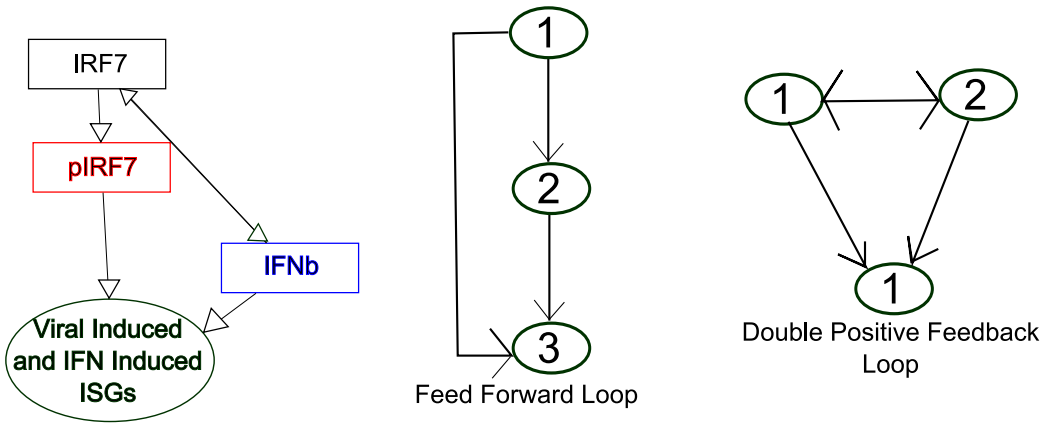

(a) IRF7-IFNβ System (b) Network Motifs

Figure 16: **IRF7 and IFNβ signaling network motifs.**

double-positive feedback loop which is defined as a feed-forward loop where the two input signals are involved in a positively reinforcing feedback loop with each other (Figure 16b). This network motif is typically associated with developmental networks, but its dominant property is that it acts as a bistable switch. In other words, the system is either completely on, completely off, or on its way towards being one of those states. Once arriving at one of those states, it is very difficult to change the state of the system.

From these two basic circuits one notes that the innate immunity circuit represented seems to serve several functions. The first is a coordination ofa rapid response to viral infection which, when given sufficient stimulus, becomes very robust and difficult to shut down, a necessary condition for combating a viral infection which may in fact be antagonizing the innate immune system. Additionally, it seems that while IRF7 coordinates the rapidity of the process (the first signal), it is IFNβ which activates the full magnitude and breadth of the innate immune response and correspondingly, is the source of the specificity component of the immune response, as a full activation of ISGs, which requires a substantial resource investment by the cell, requires multiple signals at the level of the Enhanceosome acting on the IFNβ gene and the proper signaling of IFNβ to induce the formation of ISGF3 and activate IKKε

to turns on the total array of ISGs.

It should be noted here that while the circuitry described closely resembles the two discussed network motifs, the circuitry depicted in Figure 16a is a very simplified model of the innate immune system and does not detail all the complexity of the system's behaviors. An obvious example of this would be that while the above network motifs would suspect that IFNβ stimulation would lead to greater IFNβ production due to the positive feedback loop mediated through IRF7, it is known that this is not the case (Figure 4), suggesting that there are many more actors and many more factors contributing to the topology of the innate immunity network.

However, the model is still useful to conjecture about the functional role of the division of genes according to their transcriptional regulation in Figure 15. Genes which are not IFN-dependent and not virally activated are most likely accessory components to enhance the rapidity of the first response to viral infection, but which require additional signaling in order to activate the cell's antiviral program. Genes which are virally induced most likely are the genes required for the early activation of the cell's antiviral program and help coordinate the downstream mediators which deal with committing the cell towards stably activating the antiviral program. Genes which are both virally induced and IFN-independent are the important components of the immune response that respond to the Feed Forward Loop and Double Positive Feedback loop mentioned above which are responsible for the stability and rapidity of the response. The IKKε dependent ISGs are possibly genes which are particular costly for the cell to employ and thus require the additional delay and signal guarantee of IKKε activity for their function but which show a very strong induction if the proper signals are present, while IKKε independent ISGs are genes which are required either earlier in the antiviral program and/or mediate less costly functions. The two targets of this study, TRIM30 and TRIM34, have been shown to be viral-independent and IKKε dependent ISGs of unknown function. The hypothesized model defined

above would therefore suggest that they are component of a "late" response requiring a substantial commitment and substantial upregulation by the cell post-infection. It is also possible that TRIM30 and TRIM34, as suspected E3 Ubiquitin ligases, function in the shutdown of IFN signaling. As ubiquitination is oftentimes associated with proteasomal degradation and rapid protein degradation has been observed for many activated transcription factors implicated in innate immunity, the fact that TRIM30 and TRIM34, by the model described above, are "late" response elements could suggest that they play a role in mediating a shutdown of IFN signaling which is needed for the cell to resume its normal functions.

Whether these speculations are true remains to be seen as this is of course a generalized hypothesis based on a very simplified model of the host's innate immune circuitry. Further study into the network motifs and the individual actors within innate immunity can help clarify the specific series of responses which the host cell employs to combat viral infection.

Conclusion

In closing, this study presents evidence that the transcriptional regulation of genes involved in the innate immune response can possibly present a functionally relevant subdivision of those genes based on a network-level understanding using simple network motifs. This analysis can thus be used to study genes of unknown but suspected antiviral function, such as TRIM30 and TRIM34. The evidence presented thus provides a possible insight into the role that these two proteins play in the innate immune response which will be not only of great interest to the field but towards the understanding of the cellular response to viral infection.

References

1. G. R. Stark, I. M. Kerr, B. R. Williams, R. H. Silverman, R. D. Schreiber, *Annu Rev Biochem* **67**, 227 (1998).
2. M. A. Farrar, R. D. Schreiber, *Annu Rev Immunol* **11**, 571 (1993).
3. C. E. Samuel, *Clin Microbiol Rev* **14**, 778 (2001).
4. D. B. Stetson, R. Medzhitov, *Immunity* **25**, 373 (2006).
5. S. Akira, S. Uematsu, O. Takeuchi, *Cell* **124**, 783 (2006).
6. H. Kato, *et al.*, *Nature* **441**, 101 (2006).
7. D. Thanos, T. Maniatis, *Cell* **83**, 1091 (1995).
8. W. M. Chu, *et al.*, *Immunity* **11**, 721 (1999).
9. B. R. tenOever, *et al.*, *J Virol* **78**, 10636 (2004).
10. K. A. Fitzgerald, *et al.*, *Nat Immunol* **4**, 491 (2003).
11. K. Honda, H. Yanai, A. Takaoka, T. Taniguchi, *Int Immunol* **17**, 1367 (2005).
12. T. Kawai, S. Akira, *Nat Immunol* **7**, 131 (2006).
13. M. Yoneyama, *et al.*, *Nat Immunol* **5**, 730 (2004).
14. R. B. Seth, L. Sun, C.-K. Ea, Z. J. Chen, *Cell* **122**, 669 (2005).
15. L.-G. Xu, *et al.*, *Mol Cell* **19**, 727 (2005).
16. E. Meylan, *et al.*, *Nature* **437**, 1167 (2005).
17. T. Kawai, *et al.*, *Nat Immunol* **6**, 981 (2005).
18. G. Oganesyan, *et al.*, *Nature* **439**, 208 (2006).
19. S. K. Saha, *et al.*, *EMBO J* **25**, 3257 (2006).
20. H. Hcker, M. Karin, *Sci STKE* **2006**, re13 (2006).
21. J. L. Pomerantz, D. Baltimore, *EMBO J* **18**, 6694 (1999).
22. M. Bonnard, *et al.*, *EMBO J* **19**, 4976 (2000).
23. Y. Tojima, *et al.*, *Nature* **404**, 778 (2000).
24. R. T. Peters, S. M. Liao, T. Maniatis, *Mol Cell* **5**, 513 (2000).
25. T. Shimada, *et al.*, *Int Immunol* **11**, 1357 (1999).

26. S. M. McWhirter, *et al.*, *Proc Natl Acad Sci U S A* **101**, 233 (2004).

27. H. Hemmi, *et al.*, *J Exp Med* **199**, 1641 (2004).

28. T. Decker, D. J. Lew, J. E. Darnell, *Mol Cell Biol* **11**, 5147 (1991).

29. X. Y. Fu, C. Schindler, T. Improta, R. Aebersold, J. E. Darnell, *Proc Natl Acad Sci U S A* **89**, 7840 (1992).

30. C. Schindler, X. Y. Fu, T. Improta, R. Aebersold, J. E. Darnell, *Proc Natl Acad Sci U S A* **89**, 7836 (1992).

31. B. R. tenOever, *et al.*, *Science* **315**, 1274 (2007).

32. G. Meroni, G. Diez-Roux, *Bioessays* **27**, 1147 (2005).

33. S. Nisole, J. P. Stoye, A. Sab, *Nat Rev Microbiol* **3**, 799 (2005).

34. P. S. Freemont, *Ann N Y Acad Sci* **684**, 174 (1993).

35. K. L. Borden, *et al.*, *FEBS Lett* **335**, 255 (1993).

36. K. L. Borden, *et al.*, *EMBO J* **14**, 5947 (1995).

37. M. A. Massiah, B. N. Simmons, K. M. Short, T. C. Cox, *J Mol Biol* **358**, 532 (2006).

38. A. Reymond, *et al.*, *EMBO J* **20**, 2140 (2001).

39. Z. J. Chen, *Nat Cell Biol* **7**, 758 (2005).

40. M. Stadler, *et al.*, *Oncogene* **11**, 2565 (1995).

41. J. Zhu, Z. Chen, V. Lallemand-Breitenbach, H. de Th, *Nat Rev Cancer* **2**, 705 (2002).

42. M. W. Yap, S. Nisole, J. P. Stoye, *Curr Biol* **15**, 73 (2005).

43. E. Sokolskaja, J. Luban, *Curr Opin Microbiol* **9**, 404 (2006).

44. M. Stremlau, *et al.*, *Nature* **427**, 848 (2004).

45. Y. Wang, *et al.*, *Biochem Biophys Res Commun* **323**, 9 (2004).

46. J. Zha, *et al.*, *J Immunol* **176**, 1072 (2006).

47. E. Toniato, *et al.*, *J Biol Chem* **277**, 37315 (2002).

48. W. Zou, D.-E. Zhang, *J Biol Chem* **281**, 3989 (2006).

49. W. Zou, J. Wang, D.-E. Zhang, *Biochem Biophys Res Commun* **354**, 321 (2007).

50. M. U. Gack, *et al.*, *Nature* (2007).

51. R. Patarca, *et al.*, *Proc Natl Acad Sci U S A* **85**, 2733 (1988).

52. N. Grandvaux, *et al.*, *J Virol* **76**, 5532 (2002).

53. R. Lin, P. Gnin, Y. Mamane, J. Hiscott, *Mol Cell Biol* **20**, 6342 (2000).

54. S. Ning, L. E. Huye, J. S. Pagano, *J Biol Chem* **280**, 12262 (2005).

55. K. Honda, *et al.*, *Nature* **434**, 772 (2005).

56. U. Alon, *An Introduction to Systems Biology: Design Principles of Biological Circuits* (Chapman and Hall, 2007).

57. T. Nakaya, *et al.*, *Biochem Biophys Res Commun* **283**, 1150 (2001).